Mesoporous Polymer Loading Heteropolyacid Catalysts: One-Step Strategy to Manufacture High Value-Added Cellulose Acetate Propionate

Yanfen Zhang[†#], Xiang Chen[†#], Leikai Li[†], Wei Chen[*†], Haralampos N. Miras[‡], and Yu-Fei Song[*†]

[†] State Key Laboratory of Chemical Resource Engineering, Beijing Advanced Innovation Center for Soft Matter Science and Engineering, Beijing University of Chemical Technology, Beijing 100029, P.R. China

[‡] WestCHEM, School of Chemistry, University of Glasgow, Glasgow, G12 8QQ, U.K.

Abstract

Cellulose esters are cellulose derivatives with broad application in plastics, films, fibers, coatings, textiles industries, and so forth. Taking cellulose acetate propionate (CAP) as an example, high-viscosity CAP products are widely used in printing inks, hot-melt dip coatings and lacquer coatings, and so forth. However, it was and remains to be a great challenge to manufacture high-viscosity CAP derivatives because of the overuse of sulfuric acid as catalyst that can degrade cellulose and then affect the viscosity and molecular weight of the product. Herein, with use of the copolymer of divinylbenzene with 4-vinylbenzyl chloride (PDVB–VBC) as support, imidazole-containing ionic liquid (IM) as linker, and polyoxometalates (POMs) as catalytic active sites, novel solid acid catalysts of PDVB–VBC–IM–POMs are prepared and fully characterized by Fourier transform infrared, scanning electron microscopy, transmission electron microscopy, high-resolution transmission electron microscopy, nuclear magnetic resonance, Brunauer–Emmett–Teller, thermogravimetry-differential scanning calorimetry, and X-ray photoelectron spectroscopy. Application of the as-prepared catalysts for CAP shows the following advantages: (1) high viscosity and high molecular weight (Mw) of CAP can be achieved; (2) partially substituted CAP product (degree of substitution, 2.18–2.77) can be obtained without necessity of the hydrolysis step, in which the relatively higher substitution degree of cellulose takes place at the C6 position. This work shows the great potential of new designed solid acid catalyst for high value-added cellulose derivatives.

Introduction

Cellulose is the most common biopolymer and sustainable raw material with an estimated annual natural production of 1.5×10^{12} tons.(1) Cellulose esters are cellulose derivatives with wide application in the field of plastics, films, fibers, membranes, coatings, textiles, and cigarette industries.(2−4) Cellulose esters with significant commercial value include cellulose acetate (CA), cellulose acetate propionate (CAP), cellulose acetate butyrate, and so forth. It is noted that the cellulose derivatization process is difficult in general because the natural polymer is neither meltable nor soluble in conventional solvents because of its hydrogen-bonded and partially crystallized structure.(5) Compared to many solvents, the ionic liquid systems have been extensively studied over

the past decades because of their good solubility for cellulose.(6−10)However, the recycling issue of the ionic liquids is still challenging.

Sulfuric acid is widely used as the catalyst for industrial production of cellulose esters, but serious corrosion and large amounts of wastewater can be produced. The decomposition of cellulose by sulfuric acid greatly affect the product performance including viscosity, molecular weight, and so forth.(11) Moreover, because the reaction process is very hard to control, the commonly accepted pathway in industry is that the cellulose should be fully esterified first and then be hydrolyzed to a partially substituted product. This of course necessitates a separate hydrolysis step.(11) To avoid the above issues, the solid acid catalysts have been widely investigated for cellulose derivatives.(12−15) For example, Wu and co-workers prepared the SO_4^{2-}/ZrO_2 by impregnation method using ZrO_2 as support and studied the influence on the acyl content and viscosity of CAP.(12)However, these conventional solid acid catalysts are generally not as effective as the sulfuric acid in cellulose esterification because they usually have poor accessibility or affinity to cellulose substrate because of the solid nature of both solid acid catalysts and cellulose substrate. It should be noted that Edgar and co-workers reported a new method for direct esterification of cellulose to partially substituted cellulose esters using insoluble sulfonated polystyrene resin beads as the catalyst.(13)

Polyoxometalates (POMs) are a large family of anionic metal oxides of V, Mo, W, Nb, and so forth, and have been demonstrated to be attractive catalysts for acid catalysis(16−19) and oxidation catalysis.(20−23) Indeed, a few POMs were reported for synthesis of cellulose derivatives.(24,25)For example, phosphotungstic acid was found to be an effective catalyst for the acetylation of the cellulose.(24) The CA with degree of substitution (DS) values in the range of 1.4 to 2.3 can be obtained by adjusting the amount of $H_3PW_{12}O_{40}\cdot 6H_2O$ and the time of acetylation. CA with a DS of 2.92 was obtained in the presence of sulfuric acid under identical conditions.

In this work, the polymer PDVB–VBC was designed to improve the accessibility between catalyst and substrate. The imidazole-containing ionic liquid (IM) was covalently grafted onto the polymer PDVB–VBC to enhance the solubility of cellulose during reaction. Note that POMs can slow down the decomposition of cellulose and reduce the substitution of cellulose.(11,24) As a result, the solid acid catalysts of PDVB–VBC–IM–POMs were prepared and fully characterized by Fourier transform infrared (FT-IR), scanning electron microscopy (SEM), transmission electron microscopy (TEM), high-resolution transmission electron microscopy (HR-TEM), nuclear magnetic resonance (NMR), Brunauer–Emmett–Teller (BET), thermogravimetry-differential scanning calorimetry (TG-DSC), and X-ray photoelectron spectroscopy (XPS). The experimental results showed that the molecular weight (Mw) and viscosity of CAP were largely enhanced by using PDVB–VBC–IM–POMs as catalyst Scheme 1. The ^{1}H NMR spectra suggested that the partially substituted CAP can be obtained directly without an hydrolysis step, which was unavoidable using sulfuric acid as catalyst.

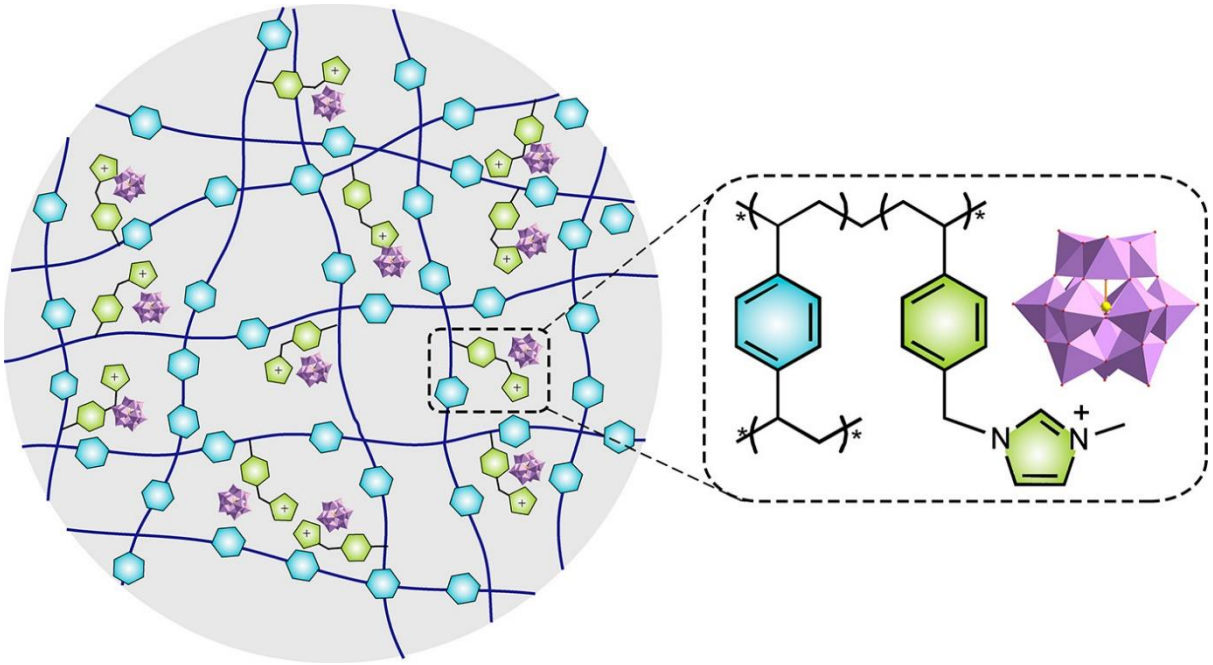

Scheme 1 - Molecular Structure of PDVB–VBC–IM–POMs Catalysts

Experimental Section

Chemical Materials

1,4-Divinylbenzene (DVB), 4-vinylbenzyl chloride (VBC), azo-bis-isobutyronitrile (AIBN), *N*-methylimidazole, *N,N*-dimethylformamide (DMF), acetone, $H_3PW_{12}O_{40}{\cdot}xH_2O$ (PW_{12}), $H_4SiW_{12}O_{40}{\cdot}xH_2O$ (SiW_{12}), $H_3PMo_{12}O_{40}{\cdot}24H_2O$ (PMo_{12}), $H_4SiMo_{12}O_{40}{\cdot}12H_2O$ ($SiMo_{12}$) were obtained from Sigma-Aldrich and were used without further treatment. Sulfuric acid, ethyl acetate, acetic acid, acetic anhydride, propionic acid, and propionic anhydride were obtained from Beijing Chemical Reagent Co., Ltd. Cellulose (degree of polymerization (DP) < 350) was obtained from Alfa Aesar.

Characterization

FT-IR spectra were recorded using KBr pellets and recorded on a NICOLET 6700 (Thermo) instrument. Solid-state NMR measurements were carried out on a Bruker Avance 300 M solid-state spectrometer equipped with a commercial 7 mm MAS NMR probe. BET measurements were performed at 77 K on a Quanta chrome Autosorb-^{1}C analyzer. The samples were degassed at 150 °C for 6 h before measurements. The ^{1}H NMR spectra were recorded on a Bruker AV400 NMR spectrometer at 400 MHz, and the chemical shifts are given relative to trimethylsilane (TMS) as internal reference. Scanning emission microscope (SEM) images were collected on a Zeiss Supra 55 VP field emission scanning electron microscope. X-ray (EDX) analytical data were obtained using a Zeiss Supra 55 SEM equipped with an EDX detector. Transmission electron microscopy (TEM) micrographs were recorded using an Hitachi H-800 instrument. TEM images were conducted on a JEOL JEM-2010 electron microscope operating at 200 kV. High-resolution TEM (HR-TEM) was performed on a JEOL JEM-2100 under an accelerating voltage of 400 kV. Thermogravimetric (TG) and differential thermal analyses (DTA) were acquired using a TG/DSC 1/1100 SF from METTLER TOLEDO under N_2 flow, heating rate of 10 °C·min^{-1}. XPS data were obtained from a Thermo-Fisher Scientific ESCALAB 250 X-ray photoelectron

spectrometer. The Mw data were obtained from a Waters 1515 GPC (gel permeation chromatograph). Viscosity of CAP was determined by an NDJ-79 rotational viscometer in a constant temperature water bath. The ultraviolet absorption spectra were recorded on a TU-1901 double-beam ultraviolet–visible spectrophotometer.

Synthesis of PDVB–VBC

PDVB–VBC and PDVB–VBC–IM were prepared and characterized according to literature method.(26−29) DVB (2.0 g) and VBC (1.5 g) were added to a solution containing 0.07 g of AIBN and 30 mL of ethyl acetate. After the mixture was stirred at room temperature for 5 h, it was hydrothermally treated at 100 °C for 24 h, followed by slow evaporation of the solvent at room temperature for 2 days. The sample designated as PDVB–VBC has monolith morphology. PDVB–VBC (1.0 g) was added to a solution containing 1.15 g of *N*-methylimidazole and 30 mL of *N*,*N*-dimethylformamide (DMF); the reaction was carried out at 80 °C for 72 h. After that, the reaction mixture was filtered, and the obtained precipitate was washed with acetone and dried at 50 °C for 12 h. The sample was designated as PDVB–VBC–IM.

Synthesis of PDVB–VBC–IM–POMs

PDVB–VBC–IM (1 g) was dispersed in 30 mL of deionized water and 4 g of PW_{12} at 60 °C for 12 h. After that, the reaction mixture was filtered and the obtained precipitate was washed with deionized water and dried at 60 °C for 5 h. The synthetic methods for PDVB–VBC–IM–PMo_{12}, PDVB–VBC–IM–SiW_{12}, and PDVB–VBC–IM–$SiMo_{12}$ were similar to that of PDVB–VBC–IM–PW_{12}.(30)

Catalytic Reaction

Acid activation of cellulose (2.0 g) should be taken into consideration, in which acetic acid (10 g), propionic acid (10 g), and a drop of H_2SO_4 (around 10 μL) were treated as activation fluids. Activation time and temperature were 1 h at room temperature. The catalyst (25 mg) and activated cellulose, as well as acetic anhydride (10 g) and propionic anhydride (10 g), were added into the reactor. The acylation was conducted at 45 °C. After 3 h, the catalyst can be separated by centrifuge. The CAP was gradually precipitated by dropping the transparent reaction solution into 5-fold deionized water. Then the CAP was filtered, washed with deionized water until odorless, and dried at 70 °C in the oven.(15)

Results and Discussion

The mesoporous polymer PDVB–VBC was synthesized by solvothermal copolymerization of DVB with VBC in ethyl acetate at 100 °C.(26) Further modification with *N*-methylimidazole and POMs led to the formation of new PDVB–VBC–IM–POMs. As shown in Figure 1a, the FT-IR spectrum of PDVB–VBC shows typical absorptions of C–Cl bond at 1260 and 670 cm^{-1}, respectively. In contrast, the FT-IR spectrum of PDVB–VBC–IM exhibits the disappearance of such C–Cl absorptions and presence of the C═N bond at 1570 cm^{-1},(26) which is consistent with its structure. For PDVB–VBC–IM–PW_{12}, the FT-IR spectrum shows strong absorption bands at 1088, 980, 920, and 810 cm^{-1}, respectively, which can be assigned to the P–Oa, W–Od, W–Oc–W, and W–Od–W asymmetric stretching vibrations, respectively.(31,32) FT-IR spectra of PDVB–VBC–IM–PMo_{12}, PDVB–VBC–IM–SiW_{12}, and PDVB–VBC–IM–$SiMo_{12}$ are shown in Figure S1 (Supporting Information).(33)

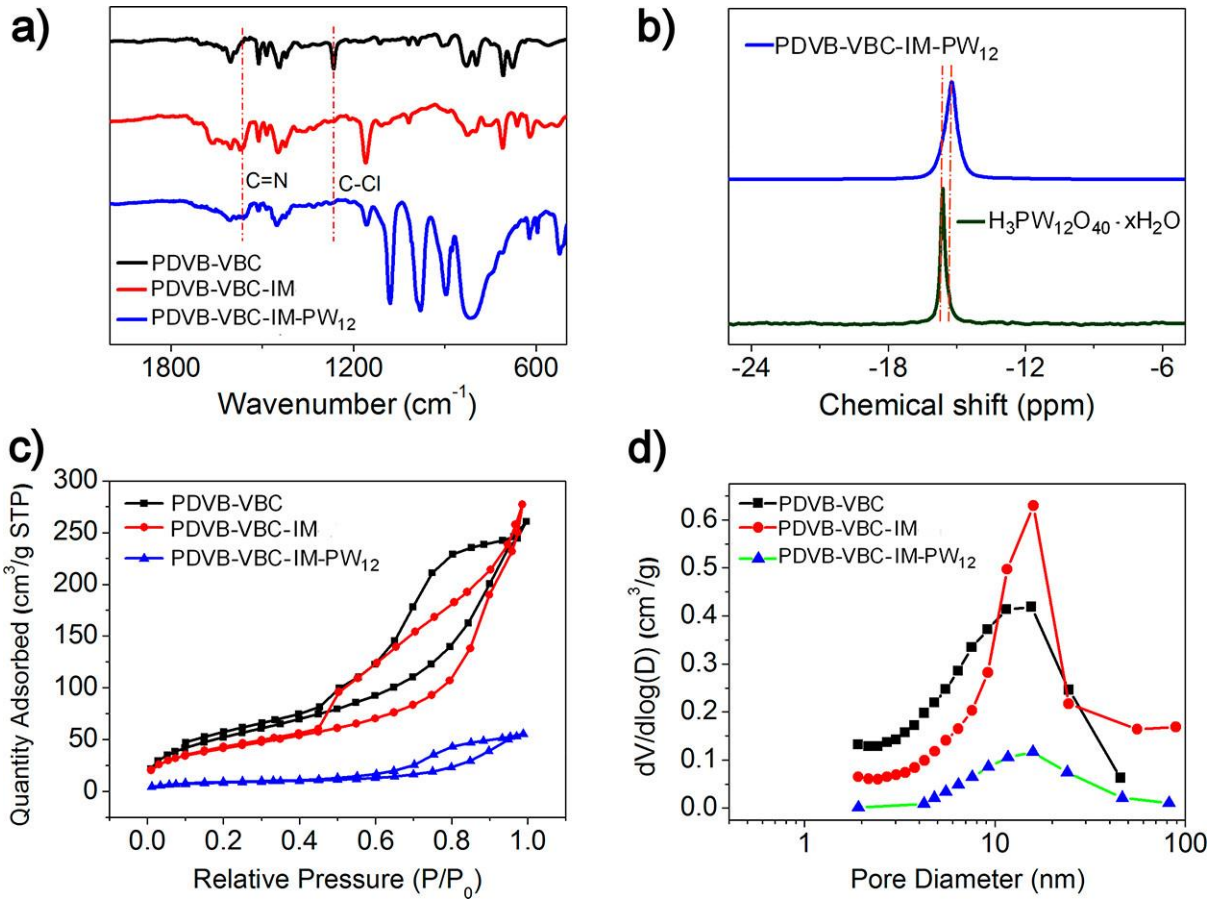

Figure 1 - (a) FT-IR spectra of PDVB–VBC, PDVB–VBC–IM, and PDVB–VBC–IM–PW_{12}, respectively. (b) ^{31}P CP/MAS NMR spectra of $H_3PW_{12}O_{40}$ and PDVB–VBC–IM–PW_{12}. (c) N_2 adsorption–desorption isotherm. (d) Pore size distribution of PDVB–VBC, PDVB–VBC–IM, and PDVB–VBC–IM–PW_{12}, respectively.

The MAS ^{13}C NMR spectra of PDVB–VBC–IM and PDVB–VBC–IM–POMs are similar (Figure S2), in which the peak around 52 ppm can be attributed to the carbon that connects the benzene ring and imidazole ring,(30) while the peak around 136 ppm is assigned to the carbon next to nitrogen on the imidazole ring.(34)

The ^{31}P MAS NMR spectrum of $H_3PW_{12}O_{40}$ (PW_{12}) exhibits a sharp peak at −15.63 ppm, while that of PDVB–VBC–IM–PW_{12} shows at peak at −15.23 ppm (Figure 1b). Such a shift can be due to the presence of the hydrogen bonding and electrostatic interactions between PW_{12} and PDVB–VBC–IM, indicating the successful preparation of PDVB–VBC–IM–PW_{12}.(26)

As shown in Figure 1, the N_2 adsorption–desorption isotherms of PDVB–VBC, PDVB–VBC–IM, and PDVB–VBC–IM–PW_{12} were classified as type IV with a clear H_1-type hysteresis loop according to the IUPAC classification, indicating the presence of mesoporosity.(35) The surface area of PDVB–VBC–IM is 150.73 $m^2 \cdot g^{-1}$. After loading of the POMs, the surface area of PDVB–VBC–IM–PW_{12} turns out to be 29.88 $m^2 \cdot g^{-1}$. The pore size distribution curves of PDVB–VBC–IM and PDVB–VBC–IM–PW_{12} can be found to be 13.06 and 11.68 nm, respectively, indicating that the regular mesoporous channels are retained in PDVB–VBC–IM–PW_{12}. TEM images and HR-TEM images are shown in Figure 2.

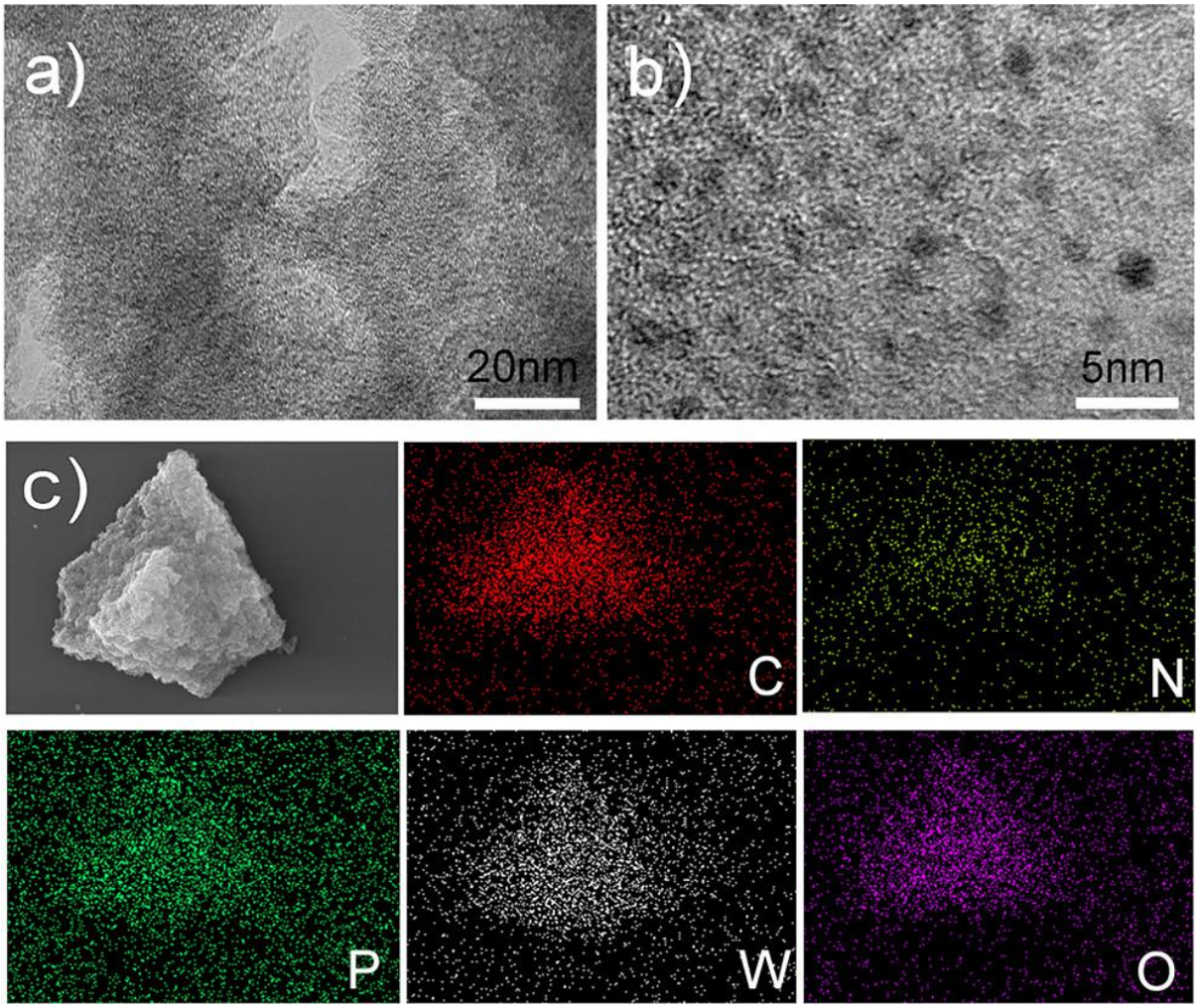

Figure 2 - TEM images (a) and HR-TEM images (b) of PDVB–VBC–IM–PW12. (c) EDS mapping of C, N, P, W, and O.

The thermogravimetric (TG) study of the PDVB–VBC–IM–PW_{12} composite (see Figure S4) performed under N_2 in the temperature range of 25–700 °C reveals three main weight losses. In the first decomposition step, the 1.25% loss in the range of 25–250 °C can be assigned to the loss of water molecules. The second weight loss of 16% between 350 and 550 °C can be attributed to the loss of the organic polymer including ionic liquid.(34) The third weight loss of 0.28% ranging from 550 to 700 °C can be due to the PW_{12}. On the basis of this result, it can be calculated that the PW_{12} loading amount is about 0.27 mmol/g for PDVB–VBC–IM–PW_{12}.

XPS measurements of PDVB–VBC–IM–PW_{12} (Figure 3) shows the C 1s peaks at 284.8, 284, and 286.2 eV associated with C═C, C–C, and C–N bonds, respectively. And the N 1s peaks at 402.0, 399.9, and 399.0 eV are associated with $C–N^+$, C–N, and $^+N–H$ bonds, respectively.(30,36) These data are in good agreement with the structure of PDVB–VBC–IM–PW_{12}. More specifically, XPS spectrum for W_{4f} (Figure 3d) reveals two peaks located at 37.6 eV of W $4f_{5/2}$ and 35.6 eV of W $4f_{7/2}$,(26,30) which are consistent with the W^{VI} oxidation state.

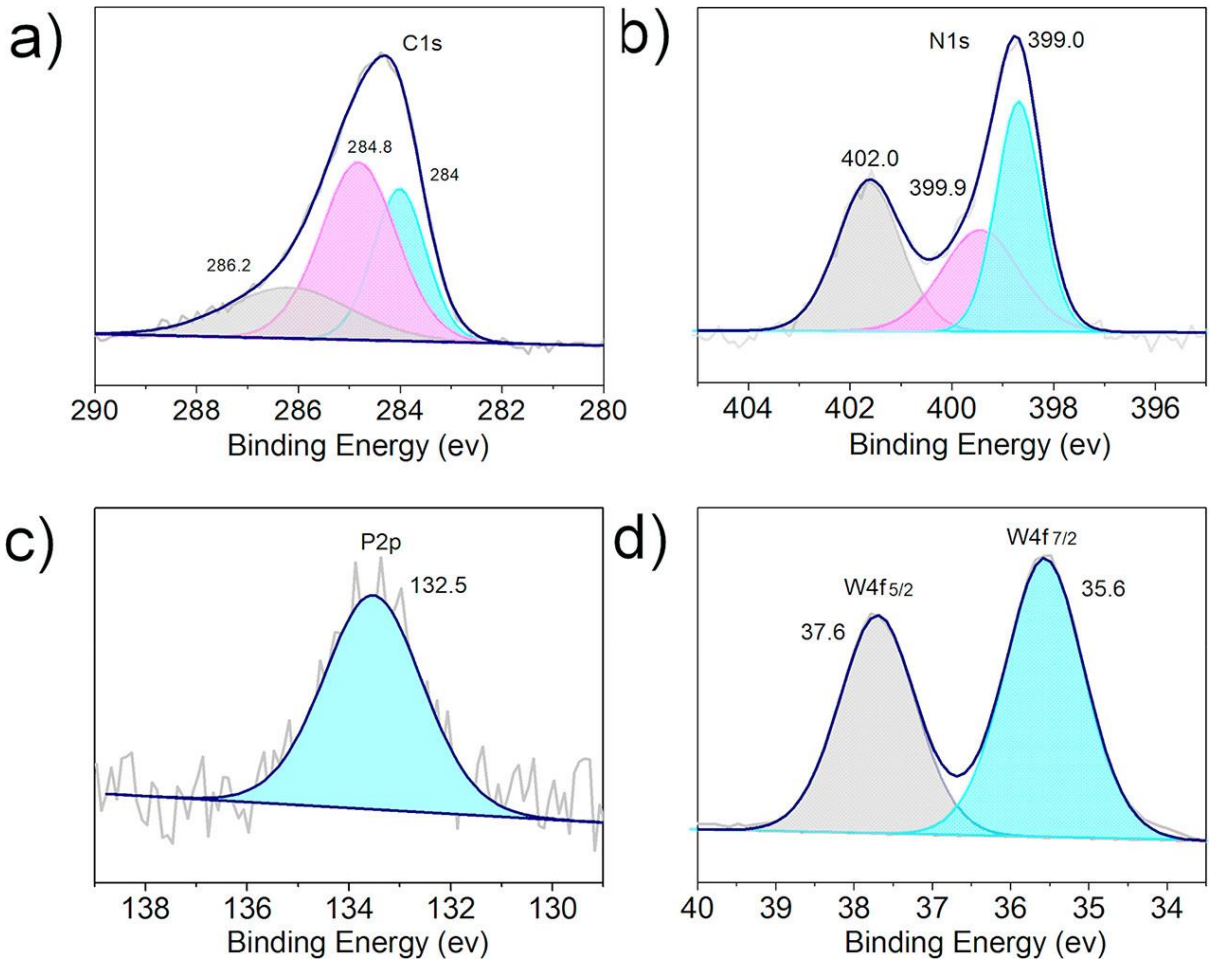

Figure 3 - XPS of PDVB–VBC–IM–PW_{12}: (a) C, (b) N, (c) P, and (d) W.

To estimate the strength and the number of acid sites present in the catalyst, the potentiometric titration with *n*-butylamine was applied. The initial electrode potential (E_i) indicates the maximum strength of the acid sites, and the value where the plateau is reached indicates the total number of acid sites present in the catalyst. The strength of the acid sites may be classified according to the following scale: $E_i > 100$ mV (very strong sites), $0 < E_i < 100$ mV (strong sites), $-100 < E_i < 0$ (weak sites), and $E_i < -100$ mV (very weak sites). The PDVB–VBC–IM–PW_{12} catalyst shows strong acid sites with E_i = 150.5 mV, while the PDVB–VBC and PDVB–VBC–IM exhibit the $E_i$value of −792.6 and −278.8 mV, respectively (Table 1).(37−39)

Table 1 - Initial Electrode Potential and Acid Density

catalyst	E_i **(mV)**	**number of acid sites (mequiv of amine/g)**
PDVB–VBC	–792.6	
PDVB–VBC–IM	–278.8	
PDVB–VBC–IM–PW_{12}	150.5	327.4

Esterification of cellulose with acetic anhydride and propionic anhydride is selected as the model reaction for the catalytic performance of the PDVB–VBC–IM–POMs solid acid catalysts (eq 1).

Chemical reaction for CAP syntheses

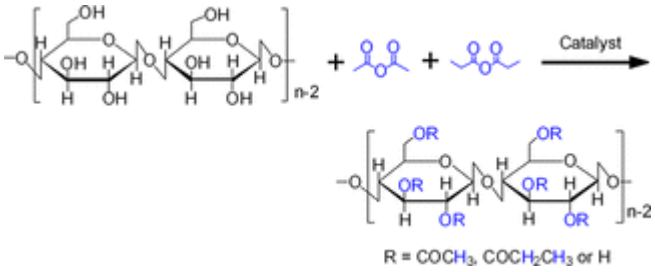

The degree of substitution (DS) indicates the degree of complete esterification of the products.(40)Table S3 shows the effect of esterification temperature on the DS and acyl content of CAP. The DS total of CAP-45 is much higher than that of CAP-40, and the DS total of CAP-50 and CAP-55 are close to that of CAP-45.

The effect of esterification temperature on the viscosity of CAP is shown in Figure 4a. The viscosity of CAP decreases with the temperature increasing from 40 to 55 °C, which can be attributed to the cellulose decomposition. The glycosidic bond on the glucose base rings in the cellulose is unstable at high temperature and under acid condition. The increase of temperature usually can promote hydrolysis and decrease the viscosity of CAP. Compared to that of the Eastman Chemical Co. commercial product CAP-482-0.5, whose viscosity is 153 mPa·s,(41,42)the viscosity of CAP catalyzed by PDVB–VBC–IM–PW_{12} is in the range of 198–498 mPa·s. Because the Mw of CAP decreases with the increase of temperature (Figure S9), the reaction temperature is optimized to be 45 °C.

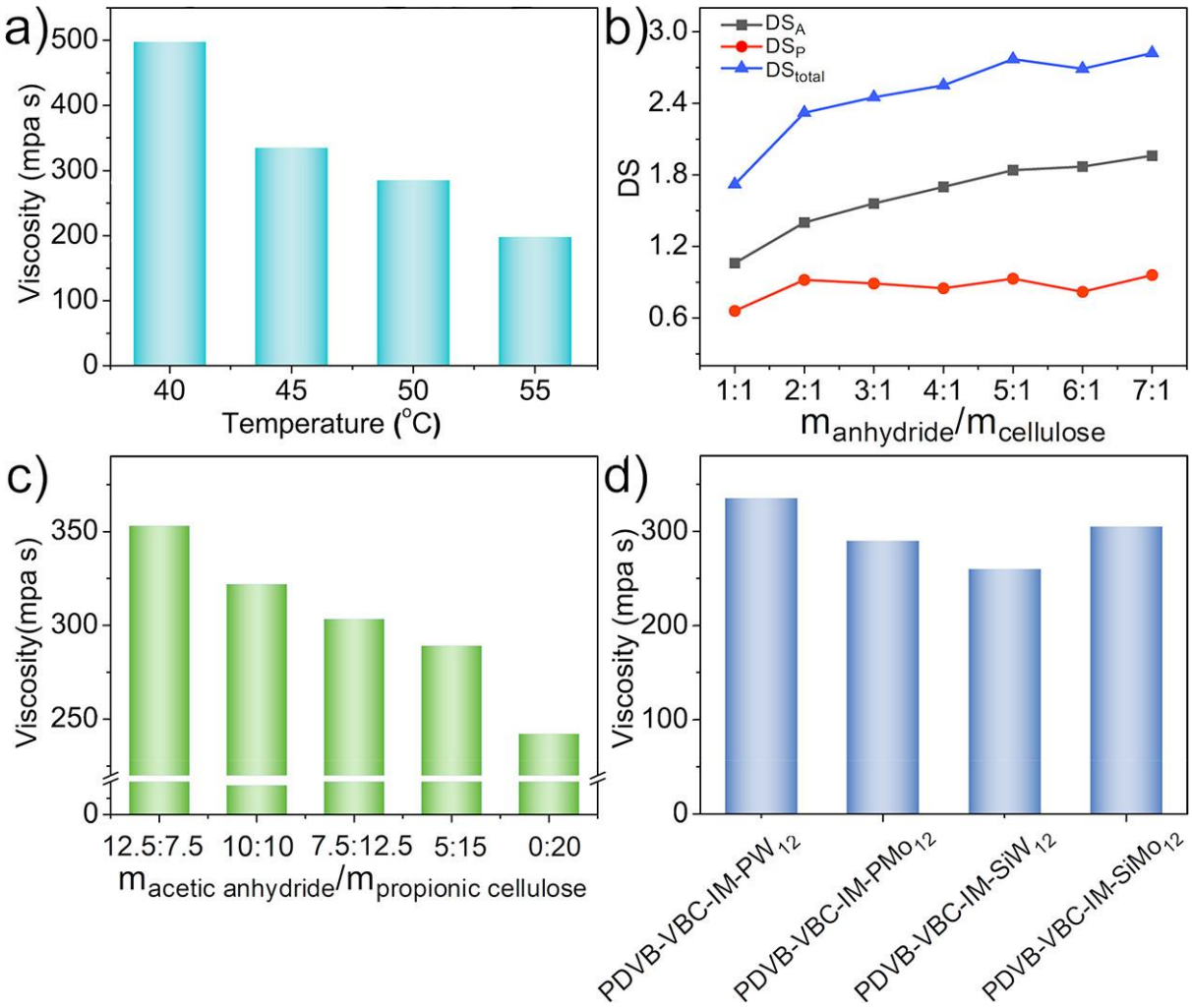

Figure 4 - (a) Effect of esterification temperature on the viscosity for CAP syntheses. Reaction conditions: 2 g of cellulose, mass ratio of esterifying agent and cellulose = 5:1, 3 h of esterification time, 25 mg of PDVB–VBC–IM–PW_{12}. (b) Effect of esterifying agent on the acyl content for CAP syntheses. (c) Effect of mass ratio of acetic anhydride and propionic anhydride on the viscosity for CAP syntheses. (d) Effect of different catalysts on the viscosity for CAP.

Table 2 shows the effect of esterification time on DS and the acyl content of CAP. With increase of the reaction time, the product DS shows a rising trend and reaches the maximum in 3 h. Then the substitution degree tends to be stable. The DS and acyl content of CAP reaches 2.77 in 3 h. Therefore, the optimum esterification time is set as 3 h.

Table 2 - Effect of Esterification Time on DS and Acyl Content for CAP Syntheses[a]

esterification time (h)	DS_A	DS_P	DS_{total}	A (%)	P (%)
1	1.11	1.13	2.24	17.55	23.69
2	1.50	1.14	2.64	22.33	22.5
3	1.84	0.93	2.77	27.16	18.19
4	1.73	0.87	2.6	26.25	17.5
5	1.78	0.83	2.61	27.02	16.7

[a] Reaction conditions: 2 g of cellulose, mass ratio of esterifying agent and cellulose = 5:1, 45 °C of reaction temperature, 25 mg of PDVB–VBC–IM–PW_{12}.

Effect of esterifying agent (acetic anhydride and propionic anhydride) on the acyl content of CAP is shown in Figure 4b. With increase of the esterifying agent, the acyl content of CAP increases accordingly. When the mass ratio of acid anhydride and cellulose is 5:1, the acyl content of CAP reaches 47.32%. As such, we select the esterifying agent and cellulose quality ratio of 5:1 for the esterification.

With increase of the propionic anhydride from 7.5 to 20 g, the viscosity of CAP decreases from 370 to 245 mPa·s. Therefore, it can be speculated that the content of propionyl group has a profound influence on the product viscosity. In another words, the higher the propyl content, the lower the product viscosity.

Effect of different catalysts on the CAP viscosity is shown in Figure 4d. The viscosity of CAP can reach 335 mPa·s by using 25 mg of PDVB–VBC–IM–PW_{12}, which is higher than that of the Eastman Chemical Co. commercial product CAP-482-0.5. In addition, the use of this method can significantly reduce the use of sulfuric acid (0.05%), compared to the use of 8–10% H_2SO_4 as catalyst in industry. Less use of

sulfuric acid greatly reduces the possibility of residual cellulose sulfonate in CAP products, increasing the thermal stability of the product.

We have performed a scaled-up experiment by using 10 times of the original experimental conditions (20 g of cellulose, 100 g of acetic acid, 100 g of propionic acid, and a drop of H_2SO_4(around 0.1 mL), 100 g of acetic anhydride, and 100 g of propionic anhydride, 250 mg of catalyst, 3 h, 45 °C). A partially substituted CAP product (DS ∼ 2.7) with high viscosity of ∼330 mPa·s and high Mw ∼ 92 500 can be obtained. The above experiments demonstrate the PDVB–VBC–IM–PW_{12} is an ideal candidate for further application.

FT-IR spectra of cellulose and CAP are shown in Figure S7. The successful acylation of cellulose is demonstrated by the presence of characteristic bands of the ester group at 1238 cm^{-1} (C–O stretching of acyl group), 1751 cm^{-1} (C═O of ester group), and the reductions in characteristic bands assigned to hydroxyl groups at 3471 cm^{-1}.(40,43)

The ^1H NMR analysis is used to evaluate the distribution of substituents (DS) and the contents of acetyl and propionyl of CAP.(44) The samples were dissolved in $CDCl_3$ containing a drop of trifluoroacetic acid-*d*, which shifts active hydrogen atoms downfield. From the ^1H NMR spectra (Figure 5a), the DS and the contents of acetyl and propionyl of CAP can be calculated on the basis of the following equations:

$$DS_A = \frac{I_{acetyl} \times 7}{I_{AGU} \times 3}$$

$$DS_P = \frac{I_{propionyl} \times 7}{I_{AGU} \times 3}$$

$$DS_{total} = DS_A + DS_P$$

$$A(\%) = \frac{DS_A \times 43}{162 - (DS_A + DS_P) + DS_A \times 43 + DS_P \times 57} \times 100\%$$

$$P(\%) = \frac{DS_P \times 57}{162 - (DS_A + DS_P) + DS_A \times 43 + DS_P \times 57} \times 100\%$$

DS_A, DS_P, and DS_{total} are the DS of the acetyl, propionyl, and acyl groups, respectively. I_{acetyl}, $I_{propionyl}$, and I_{AGU} are the peak integrals of the methyl protons of the acetyl moiety, the methyl protons of the propionyl moiety, and all protons of the anhydroglucose (AGU), respectively. The relative amounts of substituents from the three hydroxyl groups can be obtained. Peak assignment for the ^1H NMR is summarized in Table S3.(44) Furthermore, ^1H-^1H-COSY-NMR experiment clarifies the chemical shift and position of H_1 to H_6 of CAP (see in Figure 5b). It is well-known that distribution of acetyl moieties among the three OH groups of cellulose has a significant influence on the dissolution behavior of CAP.

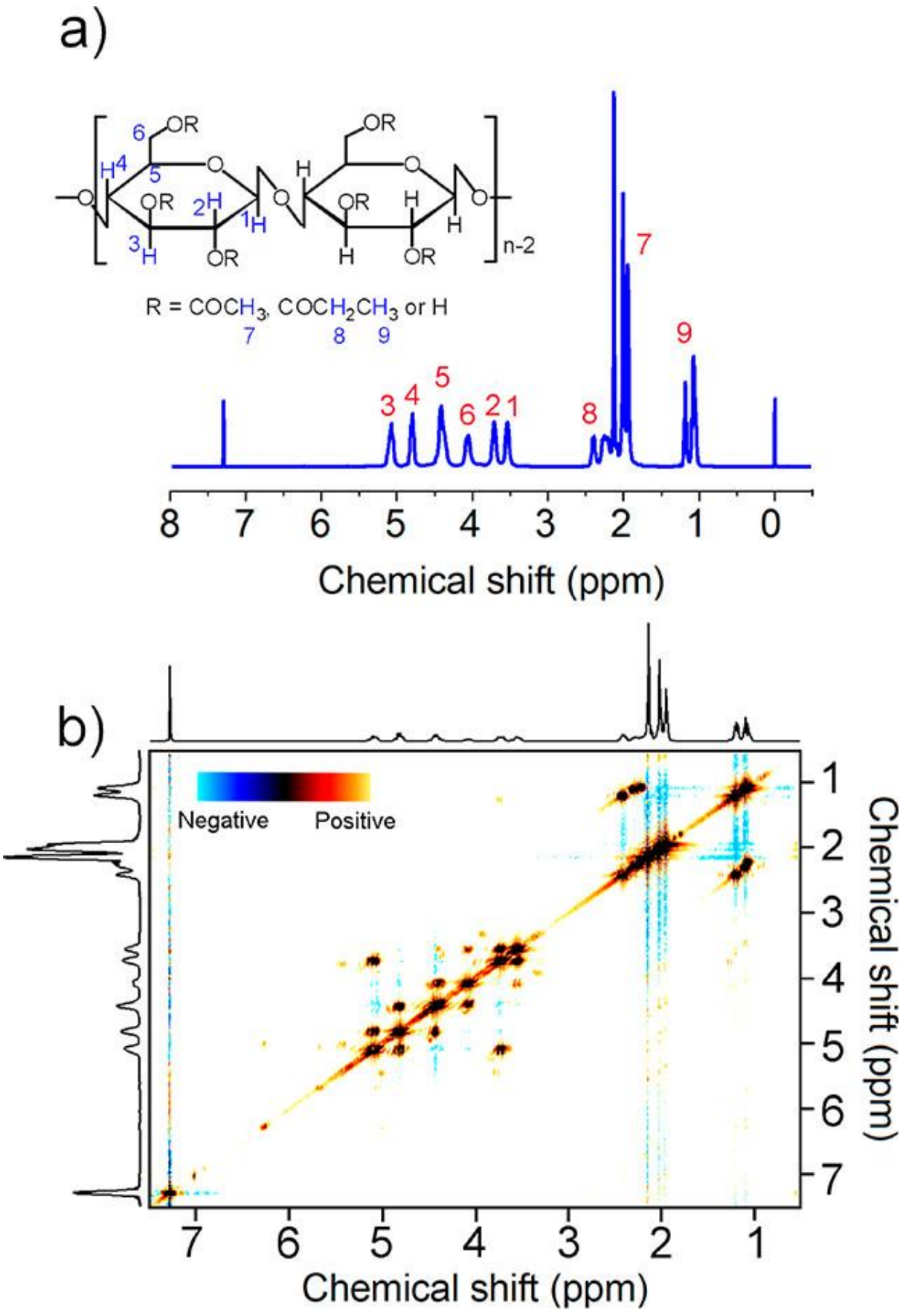

Figure 5 - (a) ^{1}H NMR spectrum and (b) ^{1}H-^{1}H-COSY-NMR spectra of the as-prepared CAP by using PDVB–VBC–IM–PW_{12} as catalyst.

The ^{13}C NMR spectrum (Figure 6) of the as-synthesized CAP confirms the distribution of acetyl moiety among three OH groups of cellulose.(40) The shifts at δ = 172.5–175.0 ppm are assigned to the signal of propionyl carbonyl carbon in CAP, and δ = 168.5–172.0 ppm are the signal of acetyl carbonyl carbon in the CAP sample. By calculating the integration of the ^{13}C NMR spectra, we can know the degree of substitution of different acyl groups at each carbon position, where the integral area ratio of the propionyl groups at different carbon positions of C_6:C_3:C_2 is 100:80:83 and that of the acetyl groups at different carbon positions of C_6:C_3:C_2 is 35:19:32. The NMR results show that the acetyl moiety among the three OH groups of the anhydroglucose unit prefers to locate at the C_6 position. It is worth noting that there are more free hydroxyls at C_6 than those at at C_2 and C_3 for partially substituted cellulose acetate prepared by commercial method because of deacetylation procedure.(45) The difference in functionalization patterns is expected to lead to the difference in solubility of CAP obtained from different path.

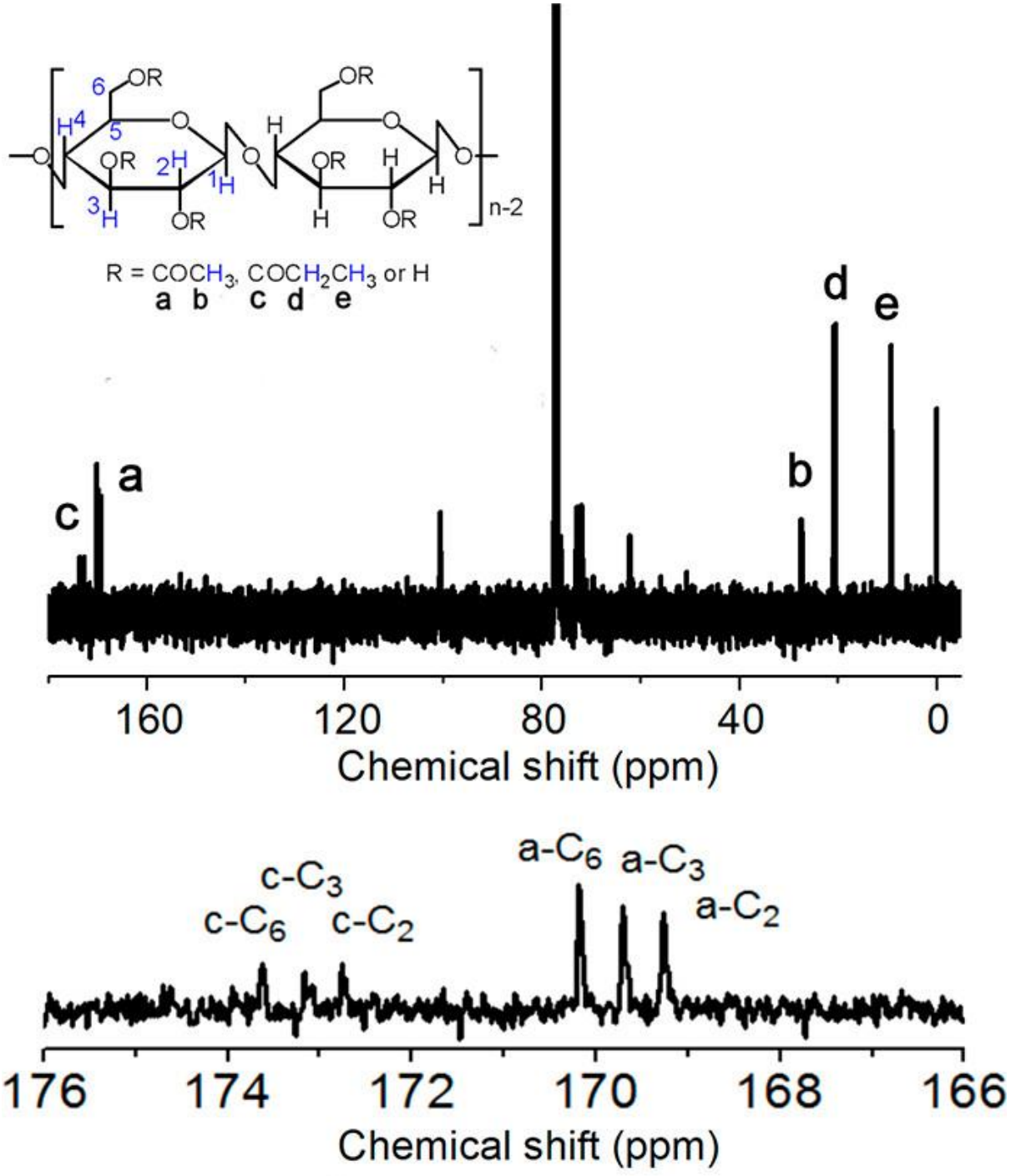

Figure 6 - ^{13}C NMR spectrum of CAP.

TG and DTA of cellulose and CAP were performed on a TG/DSC 1/1100 SF from METTLER TOLEDO under N_2 flow from 25 to 600 °C at a heating rate of 20 °C/min.(46) As shown in Figure S8a, TG of cellulose shows the decomposition in the range of 297.4–347.5 °C, while that of CAP ranges from 320.6 to 379.3 °C. It can be concluded that the thermal stability of CAP is higher than that of cellulose.

The PDVB–VBC–IM–PW_{12} can be recovered easily through centrifugation, washed with acetone, and dried at 60 °C. FT-IR spectra (Figure S12a) of the recycled PDVB–VBC–IM–PW_{12} still keep the characteristic absorption of PW_{12}. HR-TEM images (Figure S12b) results are almost the same as the

fresh one, indicating the stability of the catalyst. The catalyst can be recycled at least five times without obvious decrease of reactivity (Figure S13).

Conclusions

In this work, novel solid acid catalysts of PDVB–VBC–IM–POMs were prepared by direct copolymerization of divinylbenzene with 4-vinylbenzyl chloride (PDVB–VBC) first, followed by covalently grafting imidazole-containing ionic liquid and then electrostatically binding with POMs. The as-prepared catalysts PDVB–VBC–IM–POMs were fully characterized by FT-IR, SEM, TEM, HR-TEM, NMR, BET, TG-DSC, and XPS. Among them, partially substituted CAP product (DS = 2.18–2.77) with high viscosity of 335 mPa·s and high Mw ~ 92 500 can be achieved without the necessity of the hydrolysis step by using PDVB–VBC–IM–PW_{12} as catalyst. The resultant CAP showed high distribution of the acetyl moiety at the C_6 position. The adopted strategy herein not only reduces the use of sulfuric acid dramatically but also saves the industrial hydrolysis step and reduces the production of large amounts of wastewater. As such, this work provides a facile one-step strategy for green and clean manufacture of high value-added cellulose ester.

Supporting Information

The Supporting Information is available free of charge on the ACS Publications website at DOI: 10.1021/acssuschemeng.8b05627.

This research was supported by the National Key Research and Development Program of China (2017YFB0307303), the National Nature Science Foundation of China (U1707603, 21625101, 21521005, U1507102), the 973 program (Grant No. 2014CB932104), Beijing Natural Science Foundation (2182047), and the Fundamental Research Funds for the Central Universities (ZY1709).

The authors declare no competing financial interest.

References

(1) Klemm, D.; Heublein, B.; Fink, H. P.; Bohn, A. Cellulose: Fascinating Biopolymer and Sustainable Raw Material. Angew. Chem., Int. Ed. 2005, 44, 3358−3393.

(2) Edgar, K. J.; Buchanan, C. M.; Debenham, J. S.; Rundquist, P. A.; Seiler, B. D.; Shelton, M. C.; Tindall, D. Advances in cellulose ester performance and application. Prog. Polym. Sci. 2001, 26 (9), 1605− 1688.

(3) Fink, H. P.; Weigel, P.; Purz, H. J.; Ganster, J. Structure formation of regenerated cellulose materials from NMMO-solutions. Prog. Polym. Sci. 2001, 26 (9), 1473−1524.

(4) Schurz, J. A bright future for cellulose. Prog. Polym. Sci. 1999, 24 (4), 481−483.

(5) Cozzolino, C. A.; Cerri, G.; Brundu, A.; Farris, S. Microfibrillated cellulose (MFC): pullulan bionanocomposite films. Cellulose 2014, 21

(6), 4323−4335. (6) Pinkert, A.; Marsh, K. N.; Pang, S.; Staiger, M. P. Ionic Liquids and Their Interaction with Cellulose. Chem. Rev. 2009, 109 (12), 6712−6728.

(7) Wang, H.; Gurau, G.; Rogers, R. D. Ionic liquid processing of cellulose. Chem. Soc. Rev. 2012, 41 (4), 1519−1537.

(8) Zhao, Y.; Liu, X.; Wang, J.; Zhang, S. Insight into the Cosolvent Effect of Cellulose Dissolution in Imidazolium-Based Ionic Liquid Systems. J. Phys. Chem. B 2013, 117 (30), 9042−9049.

(9) Li, Y.; Wang, J.; Liu, X.; Zhang, S. Towards a molecular understanding of cellulose dissolution in ionic liquids: anion/cation effect, synergistic mechanism and physicochemical aspects. Chem. Sci. 2018, 9 (17), 4027−4043.

(10) Uto, T.; Yamamoto, K.; Kadokawa, J. Cellulose Crystal Dissolution in Imidazolium-Based Ionic Liquids: A Theoretical Study. J. Phys. Chem. B 2018, 122 (1), 258−266.

(11) Yang, Y.; Xie, H.; Liu, E. Acylation of cellulose in reversible ionic liquids. Green Chem. 2014, 16 (6), 3018−3023.

(12) Leng, Y.; Zhang, Y.; Huang, C.; Liu, X.; Wu, Y. Catalytic Conversion of Cellulose to Cellulose Acetate Propionate (CAP) Over SO4 2−/ZrO2 Solid Acid Catalyst. Bull. Korean Chem. Soc. 2013, 34 (4), 1160−1164.

(13) Meng, X.; Matson, J. B.; Edgar, K. J. Olefin cross-metathesis, a mild, modular approach to functionalized cellulose esters. Polym. Chem. 2014, 5 (24), 7021−7033.

(14) Zhang, C.; Fu, Z.; Liu, Y.; Dai, B.; Zou, Y.; Gong, X.; Wang, Y.; Deng, X.; Wu, H.; Xu, Q.; Steven, K. R.; Yin, D. Ionic liquidfunctionalized biochar sulfonic acid as a biomimetic catalyst for hydrolysis of cellulose and bamboo under microwave irradiation. Green Chem. 2012, 14 (7), 1928−1934.

(15) Luo, J.; Sun, Y. Acetylation of cellulose using recyclable polymeric catalysts. J. Appl. Polym. Sci. 2006, 100 (4), 3288−3296.

(16) Wang, S.; Yang, G.-Y. Recent Advances in PolyoxometalateCatalyzed Reactions. Chem. Rev. 2015, 115 (11), 4893−4962.

(17) Song, Y.-F.; Tsunashima, R. Recent advances on polyoxometalate-based molecular and composite materials. Chem. Soc. Rev. 2012, 41 (22), 7384−7402.

(18) Gaspar, A. R.; Gamelas, J. A. F.; Evtuguin, D. V.; Pascoal Neto, C. Alternatives for lignocellulosic pulp delignification using polyoxometalates and oxygen: a review. Green Chem. 2007, 9 (7), 717−730.

(19) Long, D.; Tsunashima, R.; Cronin, L. Polyoxometallate als Bausteine für funktionelle Nanosysteme. Angew. Chem. 2010, 122, 1780−1803.

(20) Leng, Y.; Wang, J.; Zhu, D.; Zhang, M.; Zhao, P.; Long, Z.; Huang, J. Polyoxometalate-based amino-functionalized ionic solid catalysts lead to highly efficient heterogeneous epoxidation of alkenes with H2O2. Green Chem. 2011, 13 (7), 1636−1639.

(21) Li, T.; Wang, Z.; Chen, W.; Miras, N.; Song, Y.-F. Rational Design of a Polyoxometalate Intercalated Layered Double Hydroxide: Highly Efficient Catalytic Epoxidation of Allylic Alcohols under Mild and Solvent-Free Conditions. Chem. - Eur. J. 2017, 23 (5), 1069− 1077.

(22) Leng, Y.; Wang, J.; Zhu, D.; Ren, X.; Ge, H.; Shen, L. Heteropolyanion-Based Ionic Liquids: Reaction-Induced Self-Separation Catalysts for Esterification. Angew. Chem., Int. Ed. 2009, 48 (1), 168−171.

(23) Li, T.; Zhang, W.; Chen, W.; Miras, H. N.; Song, Y.-F. Modular Polyoxometalate−Layered Double Hydroxides as Efficient Heterogeneous Sulfoxidation and Epoxidation Catalysts. ChemCatChem 2018, 10 (1), 188−197.

(24) Fan, G.; Wang, M.; Liao, C.; Fang, T.; Li, J.; Zhou, R. Isolation of cellulose from rice straw and its conversion into cellulose acetate catalyzed by phosphotungstic acid. Carbohydr. Polym. 2013, 94 (1), 71−76.

(25) Liu, Y.; Wang, H.; Yu, G.; Yu, Q.; Li, B.; Mu, X. A novel approach for the preparation of nanocrystalline cellulose by using phosphotungstic acid. Carbohydr. Polym. 2014, 110, 415−422.

(26) Fu, S.; Chu, J.; Chen, X.; Li, W.; Song, Y.-F. Well-Dispersed H3PW12O40/H4SiW12O40 Nanoparticles on Mesoporous Polymer for Highly Efficient Acid-Catalyzed Reactions. Ind. Eng. Chem. Res. 2015, 54 (46), 11534−11542.

(27) Dai, Z.; Sun, Q.; Chen, F.; Pan, S.; Wang, L.; Meng, X.; Li, J.; Xiao, F.-S. Enhancement of Catalytic Activity in Epoxide Hydration by Increasing the Concentration of Cobalt(III)/Salen in Porous Polymer Catalysts. ChemCatChem 2016, 8 (4), 812−817.

(28) Yue, Y.; Mayes, R. T.; Kim, J.; Fulvio, P. F.; Sun, X. − G.; Tsouris, C.; Chen, J.; Brown, S.; Dai, S. Seawater Uranium Sorbents: Preparation from a Mesoporous Copolymer Initiator by AtomTransfer Radical Polymerization. Angew. Chem., Int. Ed. 2013, 52 (50), 13458−13462.

(29) Guo, J.; Zhou, Y.; Qiu, L.; Yuan, C.; Yan, F. Self-assembly of amphiphilic random co-poly(ionic liquid)s: the effect of anions, molecular weight, and molecular weight distribution. Polym. Chem. 2013, 4 (14), 4004−4009.

(30) Liu, F.; Wang, L.; Sun, Q.; Zhu, L.; Meng, X.; Xiao, F.-S. Transesterification Catalyzed by Ionic Liquids on Superhydrophobic Mesoporous Polymers: Heterogeneous Catalysts That Are Faster than Homogeneous Catalysts. J. Am. Chem. Soc. 2012, 134 (41), 16948− 16950.

(31) Jia, Y.; Fang, Y.; Zhang, Y.; Miras, H. N.; Song, Y.-F. Classical Keggin Intercalated into Layered Double Hydroxides: Facile Preparation and Catalytic Efficiency in Knoevenagel Condensation Reactions. Chem. - Eur. J. 2015, 21 (42), 14862−14870.

(32) Chen, Y.; Yan, D.; Song, Y.-F. Tris(hydroxymethyl)- aminomethane modified layered double hydroxides greatly facilitate polyoxometalate intercalation. Dalton Trans. 2014, 43 (39), 14570−14576.

(33) Zhao, S.; Jia, Y.; Song, Y.-F. Acetalization of aldehydes and ketones over H4[SiW12O40] and H4[SiW12O40]/SiO2. Catal. Sci. Technol. 2014, 4 (8), 2618−2625.

(34) Li, D.; Li, J.; Mao, D.; Wen, H.; Zhou, Y.; Wang, J. Direct synthesis of sulfonic group tethered mesoporous poly(ionic liquid) for catalyzing deoximation reactions. Mater. Chem. Phys. 2017, 189, 118− 126.

(35) Hong, L.; Win, P.; Zhang, X.; Chen, W.; Miras, H. N.; Song, Y.- F. Covalent Immobilization of Polyoxotungstate on Alumina and Its Catalytic Generation of Sulfoxides. Chem. - Eur. J. 2016, 22 (32), 11232−11238.

(36) Win, P.; Lin, C.-G.; Long, Y.; Chen, W.; Chen, G.; Song, Y.-F. Covalently cross-linked layered double hydroxide nanocomposite hydrogels with ultrahigh water content and excellent mechanical properties. Chem. Eng. J. 2018, 335, 409−415.

(37) Romanelli, G. P.; Autino, J. C.; Blanco, M. N.; Pizzio, L. R. Tungstosilicate salts as catalysts in phenol tetrahydropyranylation and depyranylation. Appl. Catal., A 2005, 295 (2), 209−215.

(38) Rao, K. N.; Reddy, K. M.; Lingaiah, N.; Suryanarayana, I.; Prasad, P. S. A. Structure and reactivity of zirconium oxide-supported ammonium salt of 12-molybdophosphoric acid catalysts. Appl. Catal., A 2006, 300 (20), 139−146.

(39) del Rosario Torviso, M.; Alesso, E. N.; Moltrasio, G. Y.; Vazquez, P. G.; Pizzio, L. R.; Ca´ ceres, C. V.; Blanco, M. N. Effect of the support on a new metanethole synthesis heterogeneously catalyzed by Keggin heteropolyacids. Appl. Catal., A 2006, 301 (1), 25−31.

(40) Yu, Y.; Miao, J.; Jiang, Z.; Sun, H.; Zhang, L. Cellulose esters synthesized using a tetrabutylammonium acetate and dimethylsulfoxide solvent system. Appl. Phys. A: Mater. Sci. Process. 2016, 122 (7), 656.

(41) Cheng, H. N.; Dowd, M. K.; Shogren, R. L.; Biswas, A. Conversion of cotton byproducts to mixed cellulose esters. Carbohydr. Polym. 2011, 86 (3), 1130−1136.

(42) Cellulose acetate propionate product data sheet. Eastman Chemical Company, August 22, 2006.

(43) Luo, J.; Sun, Y. Acetylation of cellulose using recyclable polymeric catalysts. J. Appl. Polym. Sci. 2006, 100 (4), 3288−3296.

(44) Cao, Y.; Li, H.; Zhang, J. Homogeneous Synthesis and Characterization of Cellulose Acetate Butyrate (CAB) in 1-Allyl-3- Methylimidazolium Chloride (AmimCl) Ionic Liquid. Ind. Eng. Chem. Res. 2011, 50 (13), 7808−7814.

(45) Wu, J.; Zhang, J.; Zhang, H.; He, J.; Ren, Q.; Guo, M. Homogeneous Acetylation of Cellulose in a New Ionic Liquid. Biomacromolecules 2004, 5 (2), 266−268.

(46) Cao, Y.; Wu, J.; Meng, T.; Zhang, J.; He, J.; Li, H.; Zhang, Y. Acetone-soluble cellulose acetates prepared by one-step homogeneous acetylation of cornhusk cellulose in an ionic liquid 1-allyl-3-methylimidazolium chloride (AmimCl). Carbohydr. Polym. 2007, 69 (4), 665−672.